Tetrahedron 67 (2011) 7173–7184

Contents lists available at ScienceDirect

Tetrahedron

journal homepage: www.elsevier.com/locate/tet

Photochromism of dihydroindolizines. Part 16: Tuning of the photophysical behavior of photochromic dihydroindolizines in solution and in polymeric thin film

Saleh A. Ahmed [a,b,c,*], Zeinab A. Hozien [a], Aboel-Magd A. Abdel-Wahab [a], Shaya Y. Al-Raqa [c], Abdulrahman A. Al-Simaree [c], Ziad Moussa [c], Saleh N. Al-Amri [d], Mouslim Messali [c], Ahmed S. Soliman [d], Heinz Dürr [b]

[a] Chemistry Department, Faculty of Science, Assiut University, 71516 Assiut, Egypt
[b] University of Saarland, Fachrichtung 11.2, Organische Chemie, D-66041 Saarbrüken, Germany
[c] Chemistry Department, Faculty of Science, Taibah University, 30002 Al-Madinah Al-Mounawwara, Saudi Arabia
[d] Physics Department, Faculty of Science, Taibah University, 30002 Al-Madinah Al-Mounawwara, Saudi Arabia

ARTICLE INFO

Article history:
Received 14 March 2011
Received in revised form 13 June 2011
Accepted 24 June 2011
Available online 30 June 2011

Keywords:
Photochromism
Dihydroindolizines
1,5-Electrocylization
Kinetics
Half-lives
Temperature dependence
Solid thin film

ABSTRACT

In this work, photochromic materials based on the dihydroindolizine (DHI) system were synthesized in multistep reactions using chemical and photochemical methods. Some of the synthesized photochromic dihydroindolizine derivatives were substituted on the fluorene (region A) and pyridazine (region C) moieties in order to provide the appropriate functionality for optimal tuning of the photochromic properties of the system. Irradiation of the photochromic DHIs with polychromatic light led to ring opened colored betaines, which underwent thermal 1,5-electrocyclization. The red to green colored betaines produced after UV irradiation returned back through 1,5-electrocyclization to the corresponding DHIs with different rate constants depending on the substituents in both fluorene and pyridazine regions. The kinetic measurements of the thermal 1,5-electrocyclization under different temperatures that ranged from −10 to 25 °C showed that the half-lives of the colored betaines fall in the second to hours domain. Interestingly, these materials showed a very good photochromic behavior not only in solution but also in the PMMA matrix. Irradiation of a slide prepared by the deep-coating method led to the formation of the colored betaine and the kinetics of the thermally reversible 1,5-electrocyclization and the AFM image of the film has been recorded. Indeed, the chemical and thermal stability of the investigated betaines in polymer (PMMA) will render such species useful for a plethora of new of applications.

1. Introduction

Today, the photochromism phenomenon, a branch of photochemistry, has gained much momentum as it found many proven applications relevant to modern daily life.[1] Further, it is anticipated to be the basis in the development of numerous upcoming novel applications. The widely accepted definition of photochromism is the reversible absorption change exhibited by systems irradiated using light of suitable wavelength.[1–3] The reversible change of color is the main characteristic of this phenomenon, bestowing uniqueness to the transformation compared to other photoinduced reactions. The thermal or illumination reversibility of these materials configures the fascinating ability of modulating given physical properties through an external stimulation, namely, upon light irradiation.[4–9] The most characteristic properties of the materials to find pronouncing applications are: (i) the ease and fast ability to be activated by sunlight and bleached through a thermal or other wavelength, (ii) wide-range absorption in the visible region to provide different color upon irradiation, (iii) a suitable fading rate, which is related to the stability of the colored state, (iv) high efficiency of coloration upon irradiation (colorability), and (v) a high resistance to photodegradation (photofatigue-resistance).[10–12] Photochromic dihydroindolizines (DHIs) and tetrahydroindolizines (THIs) were discovered and devolved by Dürr in 1979,[13,14] they became very interesting classes of photochromic molecules and received particular attention owing to their remarkable photofatigue-resistance and broad photochromic properties.[15–20] They have already found applications in optical technology,[18a] ophthalmic lenses,[19] data storage,[20] photoswitches,[21] dental filling materials,[22,23] IR-sensitive photoswitchable

* Corresponding author. E-mail address: saleh_63@hotmail.com (S.A. Ahmed).

0040-4020/$ – see front matter © 2011 Elsevier Ltd. All rights reserved.
doi:10.1016/j.tet.2011.06.092

materials,[24] and DNA markers.[25] Such molecules undergo a photoinduced change of color in solutions and in polymer matrices when exposed to UV radiation or direct sunlight exposure and return to the initial state when the illumination ceases, normally via a thermal pathway. The photochromic behavior of DHIs (Fig. 1) is based on a reversible pyrroline ring opening, induced by light, which converts a colorless form (usually named the 'closed form') to the colored form (betaine form).[15–25] The thermal back reaction- the 1,5-electrocyclization- from the ring open betaine to DHI shows rates extending from milliseconds to several weeks depending on the substituents and structure of the molecule involved.[20–26] This interesting wide range in the lifetime of the colored form leads these molecules to find many versatile applications.[13–26]

In continuation of our previous work dealing with the synthesis and photochromic properties of dihydroindolizines (DHIs),[20–26] we now report the synthesis and photochromic properties of dihydroindolizines bearing substituted fluorene (region A) and pyridazine moiety in region C (Fig. 1). The existence of fluorene in the DHI skeleton has advantages since the fluorene is a very stable planar unit, which is widely used in optoelectronic materials.[27] The present studies of their photochromic behavior in both solution and solid thin film (PMMA) matrix as dopants. Also, the temperature dependence of the 1,5-electrocyclization to obtain different fading rates to suit some industrial applications is the main motivation behind this work.

2. Results and discussion

2.1. Synthesis of thermally reversible photochromic DHIs 3a–f containing substituted fluorene (region A) and substituted pyridazine (region C) moieties

The photochromic dihydroindolizines DHIs **3a–f** (Scheme 1) were obtained via a modified cyclopropene route (Scheme 1).

When spirocyclopropenes **1a–c** were allowed to react with substituted pyridazines **2a–d** in dry ether and in the absence of light under an atmosphere of nitrogen for 24 h, the desired photochromic dihydroindolizines **3a–f** (Table 1) were obtained in 27–40% yields as pale to yellow crystalline form after recrystallization from the proper solvent.

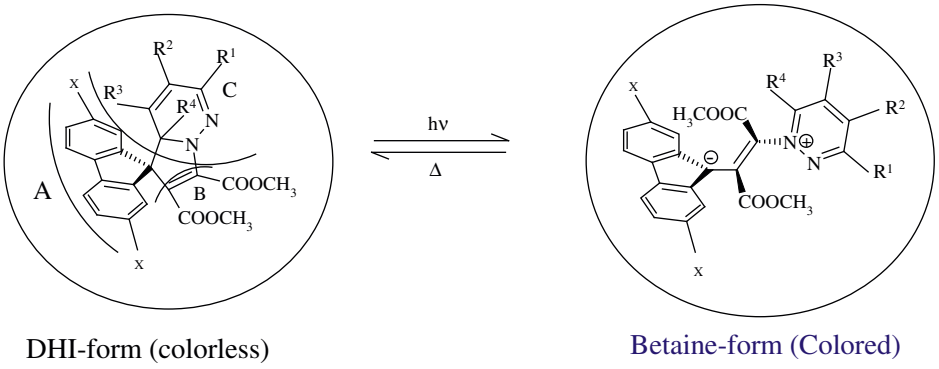

Fig. 1. Representation of the colorless (closed form) and the colored (betaine form) of dihydroindolizines.

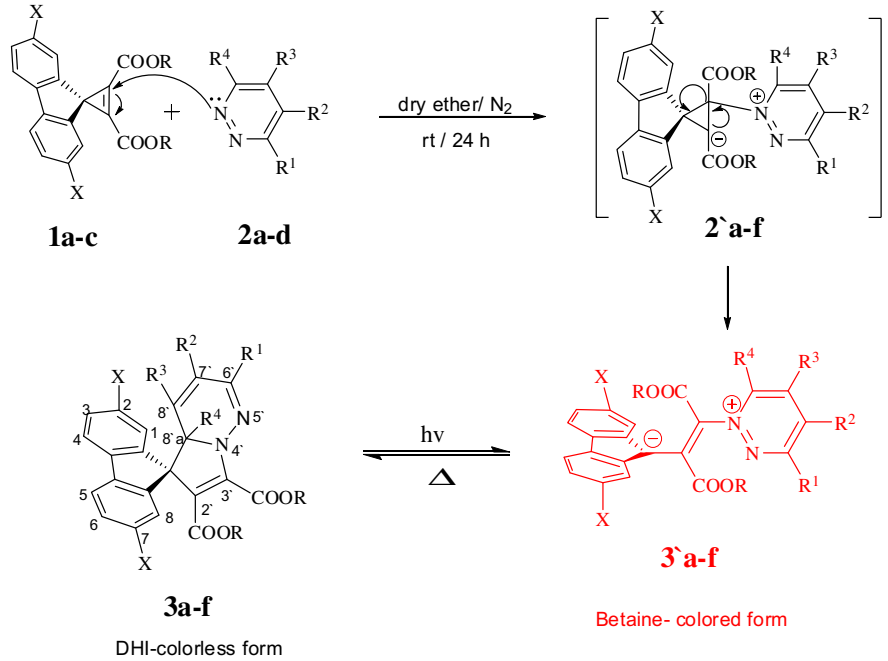

Scheme 1. Synthesis and mechanism of formation of DHIs **3a–f** and their corresponding betaine **3′a–f** via a modified spirocyclopropene route.

Table 1
Substitution pattern of the synthesized DHIs **3a**–**f**, reaction yields, and melting points

3/3′	X	R	R_1	R_2	R_3	R_4	Yield %	mp (°C)
a	H	CH_3	H	H	H	H	40	125
b	H	CH_3	CH_3	H	H	H	43	190
c	H	CH_3	C_7H_{15}	H	H	CH_3	27	121
d	Cl	CH_3	H	H	H	H	38	128
e	Br	CH_3	H	H	H	H	35	135
f	Br	CH_3	CH_3	CH_3	CH_3	CH_3	29	165

The pure products were obtained after being subjected at least twice to purification by column chromatography on silica gel using dichloromethane as eluent.

The reaction mechanism (Scheme 1) could be rationalized through the electrophilic addition of the electron-deficient and strained spirocyclopropenes **1a**–**c** to the nitrogen atom of the *N*-heterocyclic pyridazines **2a**–**d**, which leads to ring opening via a cyclopropyl-allyl conversion of **2′a**–**f** to the colored betaines **3′a**–**f** (Scheme 1). A subsequent ring-closure to DHIs **3a**–**f** resulting from slow thermal 1,5-electrocyclization (Scheme 1), which can be reversed upon exposure to light.

2.2. Characterization of the synthesized photochromic DHIs 3a–f

In order to establish and confirm the structures, stereochemistry, and position of heteroatoms, extensive ^1H, ^{13}C, DEPT 135, and correlation NMR (^1H–^1H COSY and ^1H–^{13}C COSY) spectrometry experiments were conducted in $CDCl_3$ and are tabulated in Tables 1 and 2 of the Supplementary data section for **3b** and **3c** and summarized in the Experimental section for all compounds. Thus, the structures for all synthesized photochromic compounds **3a**–**f** were assigned and further confirmed by other spectroscopic and analytical tools. For example, the Dept-135 spectrum of DHI **3c** (see Supplementary data) showed 14 signals with positive phases corresponding to the 8CH-carbons of the fluorene moiety at δ 128.2, 128.1, 127.0, 126.9, 126.6, 124.8, 120.0, and 119.7 ppm. The pyridazine carbons appeared at δ 133.4 ppm for 8′-CH and at 117.6 ppm for 7′CH, whereas signals for the methyl carbons appeared at δ 53.1 (3′-CH_3), 50.9 (2′-CH_3), 22.5 (8′a-CH_3), and 14.1 (6′g-CH_3) ppm. On the other hand, signals with negative phases characteristic of the methylene carbons appeared with chemical shifts as follows: δ 34.9 (6′a-CH_2), 31.7 (6′b-CH_2), 29.1 (6′c-CH_2), 29.0 (6′d-CH_2), 27.1 (6′e-CH_2), 22.6 (6′f-CH_2) ppm.

From the ^1H NMR, HSQC, and HMBC (showing distinctive long-range cross peaks between 8′a-CH_3 at δ 1.56 ppm and 8′a-C at δ 71.0 ppm and *C*-spiro at δ 66.2 ppm; also characteristic contours are noted between 8′-CH_3 at δ 0.73 ppm and 8′a-C at δ 71.0, 8′-C at δ 138.5, and 7′-C at δ 122.7 ppm; see Supplementary data) data, it is interesting to note that the 8′-CH_3, while being mindful of its sp^2 hybridization, has been significantly shifted to a higher field, which may be partially attributed to the anisotropic effect of the fluorene moiety. The upfield shift is in good agreement with molecular mechanics calculations (Fig. 2), which show the methyl lying under or in close proximity to the shielding zone of the fluorene moiety and is forced into such position due to the rigid and orthogonal nature of the pyridazine and fluorene moieties (Fig. 2). More spectroscopic details about all NMR data are cited as Supplementary data.

2.3. Photophysical properties of photochromic DHIs 3a–f and their corresponding betaine 3′a–f

*2.3.1. Absorption spectra of DHIs **3a–f** and their corresponding betaines **3′a–f** in dichloromethane ($c=1\times10^{-4}$ mol/L) at ambient temperature.* The photophysical data pertinent to the photochromic properties of DHIs **3a**–**f** were obtained from their absorption profiles. Thus, the absorption spectra of the synthesized DHIs **3a**–**f** were measured in dichloromethane using a UV–vis spectrophotometer with a concentration of 1×10^{-4} mol/L at ambient temperature. The photochromic DHIs **3a**–**f** showed a pale to yellow color in dichloromethane solution as well as in the solid state (Table 4). The band absorption intensities ($\log \varepsilon$) of these compounds were found to range between 3.86 and 4.79 depending on the substituents on both, the fluorene (region A) and pyridazine (region C) moieties.

The absorption maxima of the DHIs **3a**–**f** were observed in the middle UV-region and ranged between 386 and 395 nm (Fig. 3, Table 2). A very small hypsochromic shift by 3 nm was observed by substituting the 2,7-positions of the non-substituted fluorene in **3a** to give the 2,7-dibromosubsituted fluorine **3e**. On the other hand, introducing methyl and heptyl substituents to the non-substituted pyridazine region of DHIs **3a** and **3b** are essentially the same

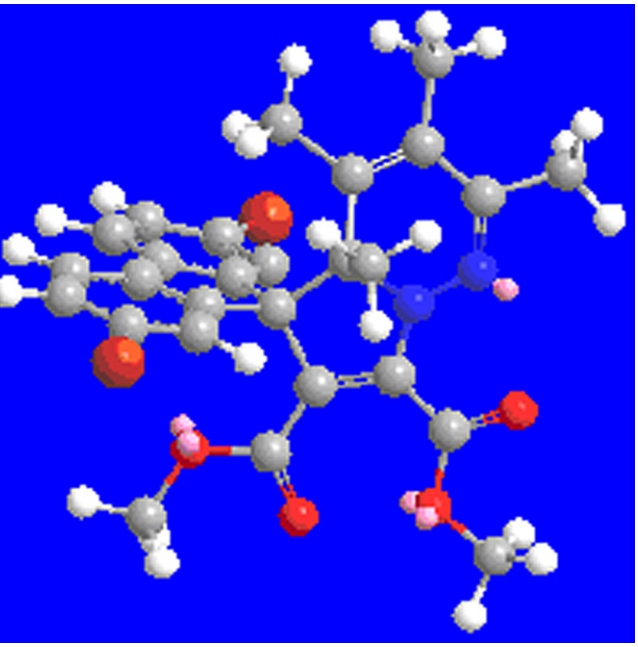

Fig. 2. Representation of the optimized (MM2) structure of DHI **3f**.

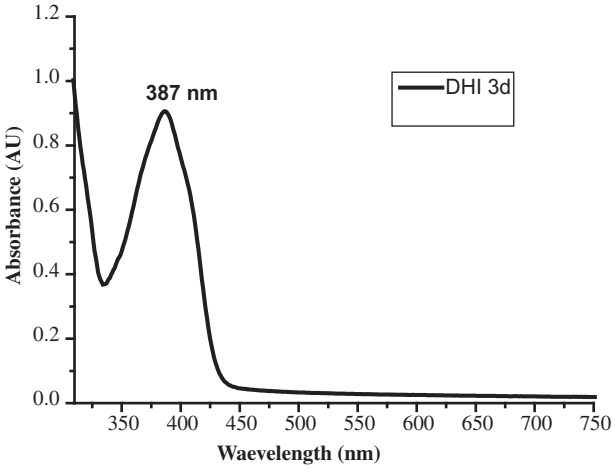

Fig. 3. UV–vis-spectrum of DHI **3d** in CH_2Cl_2 ($c=1\times10^{-4}$ mol/L) at ambient temperature.

Table 2
Absorption spectral data of DHIs **3a**–**f** and their corresponding betaines **3′a**–**f** and kinetic data of betaines **3′a**–**f** in the sec range (monitored by UV-spectrophotometer) in CH_2Cl_2 solution ($c=1\times10^{-4}$ mol/L) at ambient temperature

DHI/Betaine	λ_{max} (DHI) [nm]	log (ε)	λ_{max} (Betaine) [nm]	Color of betaine
3a/**3′a**	389	4.06	340, 517	Red
3b/**3′b**	388	3.86	522	Red-Violet
3c/**3′c**	395	4.70	346, 443, 628	Green
3d/**3′d**	387	4.79	346, 528	Violet
3e/**3′e**	386	4.23	538	Violet
3f/**3′f**	391	4.13	447, 623	Blue-Green

whereas for DHI **3c** exhibited bathochromic shift. These absorption bands can be assigned to the locally excited π–π*-transition (LE) located in the butadienyl-vinyl-amine chromophores[1,20–26] of the DHIs **3a**–**f** (Table 2).

Polychromatic light irradiation of DHIs **3a**–**f** generated ring opened betaines **3′a**–**f** (Table 2, Fig. 4). The colored betaine forms **3′a**–**f** varied from red to blue-green in CH_2Cl_2 with a concentration of 1×10^{-4} mol/L at room temperature because of their slower 1,5-electrocyclization. All the absorption maxima of the colored betaines **3′a**–**f** were found to be in the visible region and lie between 517 (betaine **3′a**) and 628 nm (betaine **3′c**).

The UV–vis absorption spectra of the colored betaines **3′a**, **d**, **e** (Figs. 4 and 5) containing a non-substituted pyridazine as a heterocyclic moiety in region C exhibited a red to red-violet colored betaine forms and showed one to two absorption maxima ranging between 517 and 538 nm (Figs. 4 and 5). On the other hand, the betaine **3′b**, which contains a methyl substituent in region C exhibited a red-violet colored betaine form (λ_{max}=522 nm), while the dialkyl substituted betaine **3′c** showed a dark green color and three

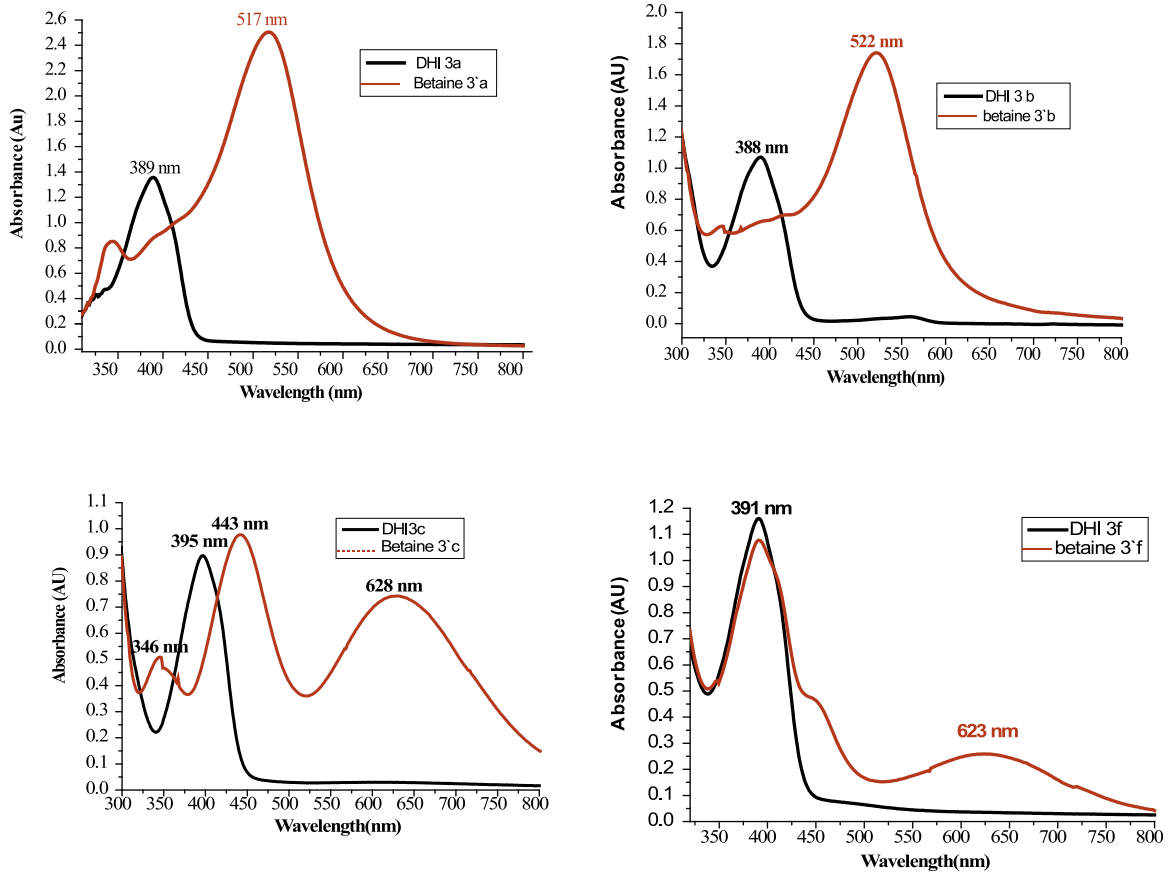

Fig. 4. UV–vis spectra of DHIs **3a**, **b**, **c**, **f** and their corresponding betaines **3′a**, **b**, **c**, **f** at 25 °C (except betaine **3′f** at 10 °C due to the fast thermal back reaction) in CH_2Cl_2 solution ($c=1\times10^{-4}$ mol/L).

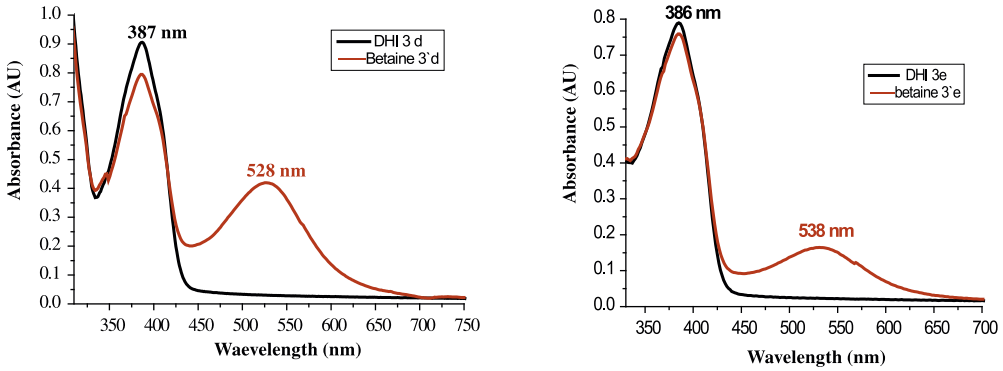

Fig. 5. UV–vis spectra of DHIs **3d**, **e** and their corresponding betaines **3′d**, **e** in CH_2Cl_2 solution ($c=1\times10^{-4}$ mol/L) at 25 °C.

absorption maxima at 628, 443, and 346 nm (Table 2, Fig. 4) along with three isosbestic points. In addition, betaine **3′f**, which is tetra-substituted with methyl groups on the pyridazine moiety showed blue-green color with absorption maxima at 623 and 447 nm (Fig. 4). The existence of three isosbestic points clearly suggests that the thermal back reaction of the colored betaines follows first order. Interestingly, a bathochromic shift in the absorption of the betaines containing non-substituted pyridazines **3a**, **d**, **e**, by more than 115 nm in the visible region is noted compared to the alkyl-substituted pyridazines **3c**, **f** (Fig. 4). The large bathochromic shift leading to the change of the colored forms from red to blue-green and absorptions in the visible region has been attributed to the increase in the electron donating ability of the alkyl groups, which imparts stability to the zwitter ionic betaine forms (Table 2).

Furthermore, a noticeable bathochromic shift of about 21 nm was observed when dichloro- and dibromo-substituents were introduced on the fluorene moiety (region A) of the non-substituted betaine **3′a** (Fig. 4) to generate dichloro betaine **3′d** and dibromo betaine **3′e** (Fig. 5). From Fig. 5, it is clear that a faster thermal back reaction is associated with the dibromo-substituted betaine **3′e** compared to the dichloro analogue **3′d** as the former exhibits higher absorbance. More detailed UV–vis spectroscopic data of the colored betaines is listed in Table 2 and graphically represented in Figs. 4 and 5.

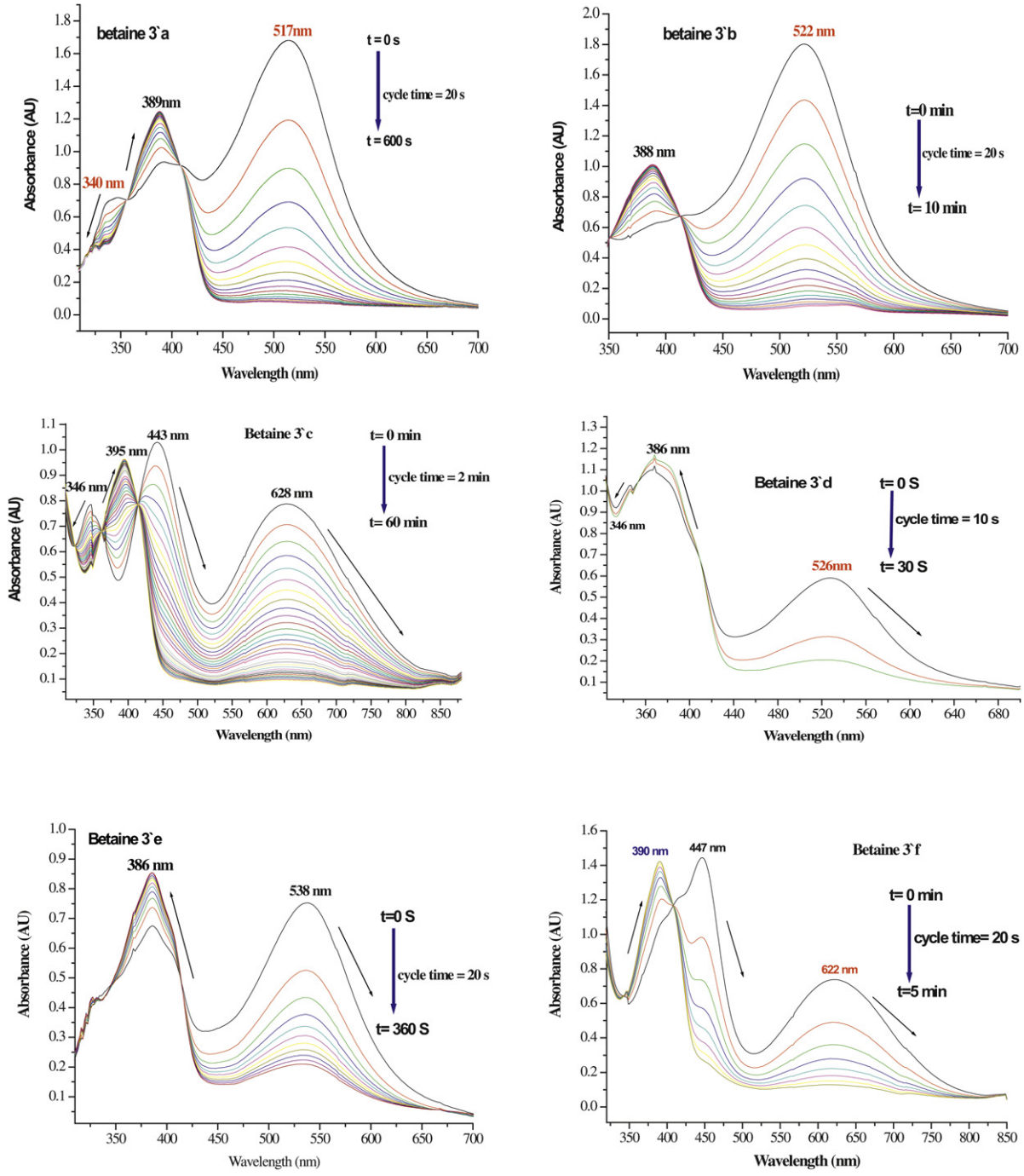

Fig. 6. Scan kinetic spectra of the thermal fading of betaines **3′a**–**f** to DHIs **3a**–**f** (cycle time and run time are cited inside the figures in CH_2Cl_2 (c=1×10^{-4} mol/L) at 25 °C; betaine **3′e** and **3′f** were measured at 0 °C because of higher betaine concentration).

*2.3.2. Kinetics of the thermally reversible 1,5-electrocyclization of the betaine **3′a–f** to their corresponding DHIs **3a–f** in dichloromethane solution.* In order to examine the photochromic behaviors of the DHIs and betaines in solution, kinetic measurements were undertaken using UV–vis spectroscopy. DHIs are divided into five major categories depending on the cyclization rate constant (k), which is the main factor for determining the half-lives of the colored form.[20–26] These categories can be summarized as follows:

(i) Very slow systems ($t_{1/2}$<1 h)
(ii) Slow systems ($t_{1/2}$<1 min)
(iii) Middle systems (1 s>$t_{1/2}$>1 min)
(iv) Fast systems (1 ms>$t_{1/2}$>1 s)
(v) Very fast systems ($t_{1/2}$>1 ms).

These categories give a special meaning to the measurement techniques employed. The first three categories can be easily examined at room temperature with normal UV–vis photospectrometer. The rate constants of the thermally reversible 1,5-electrocyclization of betaines were determined at constant temperature by measuring the decrease in the maximum absorption intensity (λ_{max}) with time. The half-lives ($t_{1/2}$) and rate constants (k) of betaines under examination were calculated by plotting lnA against time (t). In agreement with reported literature results,[1,20–26] the thermal 1,5-electrocyclization of the investigated compounds followed a first-order mechanism. The $t_{1/2}$ of betaines **3′a–f** could be determined by UV–vis spectrophotomer because of their low cyclization rate constant (k). The decay of the absorption curves of betaines **3′a–f** followed a first order mechanism. According to the first order mechanism:

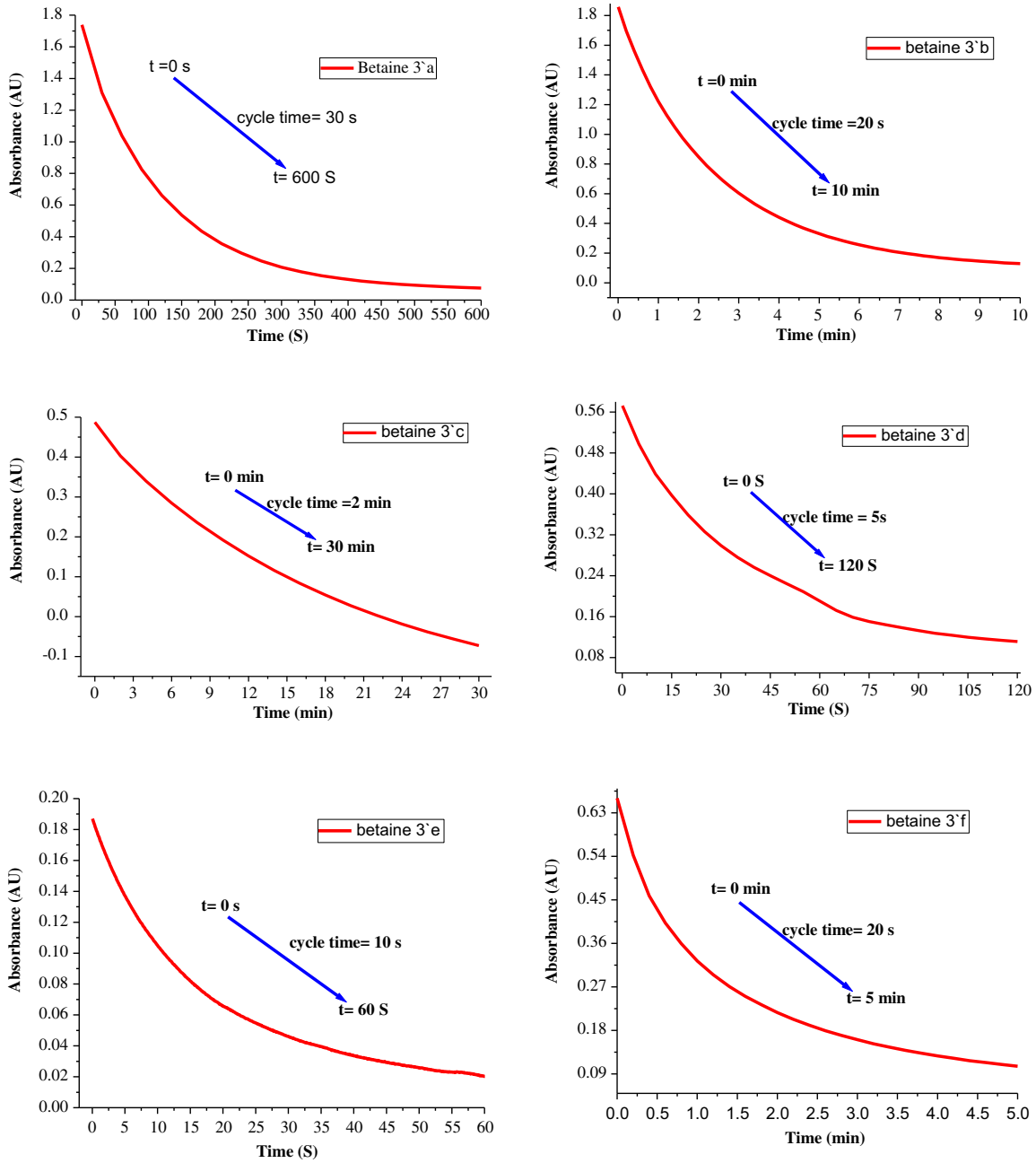

Fig. 7. Absorbance–time relationship for the kinetic thermal fading of betaines **3′a–f** to DHIs **3a–f** for determination of the thermally reversible 1,5-electrocyclization rate constant (k) in CH_2Cl_2 solution (c=1×10^{-4} mol/L).

$$-dC_{betaine}/dt = k \times C_{betaine} \quad (1)$$

From Beer–Lambert law:

$$E = \varepsilon \times c \times d \quad (2)$$

Substituting Eq. 1 in Eq. 2 yields:

$$-dE_{betaine}/dt = k \times E_{betaine} \quad (3)$$

Integration of Eq. 3 and simplification gives:

$$\ln E = \ln E_0 - kt \quad (4)$$

where k is the reaction rate constant for the thermally reversible 1,5-electrocyclization.

From the decay curves, the half-lives of the betaine forms 3′a-f were calculated as cited in Table 3 by applying Eq. 5.

Table 3
Kinetic data of the thermally reversible 1,5-electrocyclization of betaine **3′a–f** to their corresponding DHIs **3a–f** in CH_2Cl_2 solution (25 °C, $c=1\times10^{-4}$ mol/L)

DHI/Betaine	kx10^{-3} (s^{-1})	$t_{1/2}$ (s)
3a/3′a	6.76	102
3b/3′b	2.77	250
3c/3′c	0.25	2700
3d/3′d	10.34	67
3e/3′e	16.12	43
3f/3′f	3.61	192

$$k = \ln 2/t_{1/2} \quad (5)$$

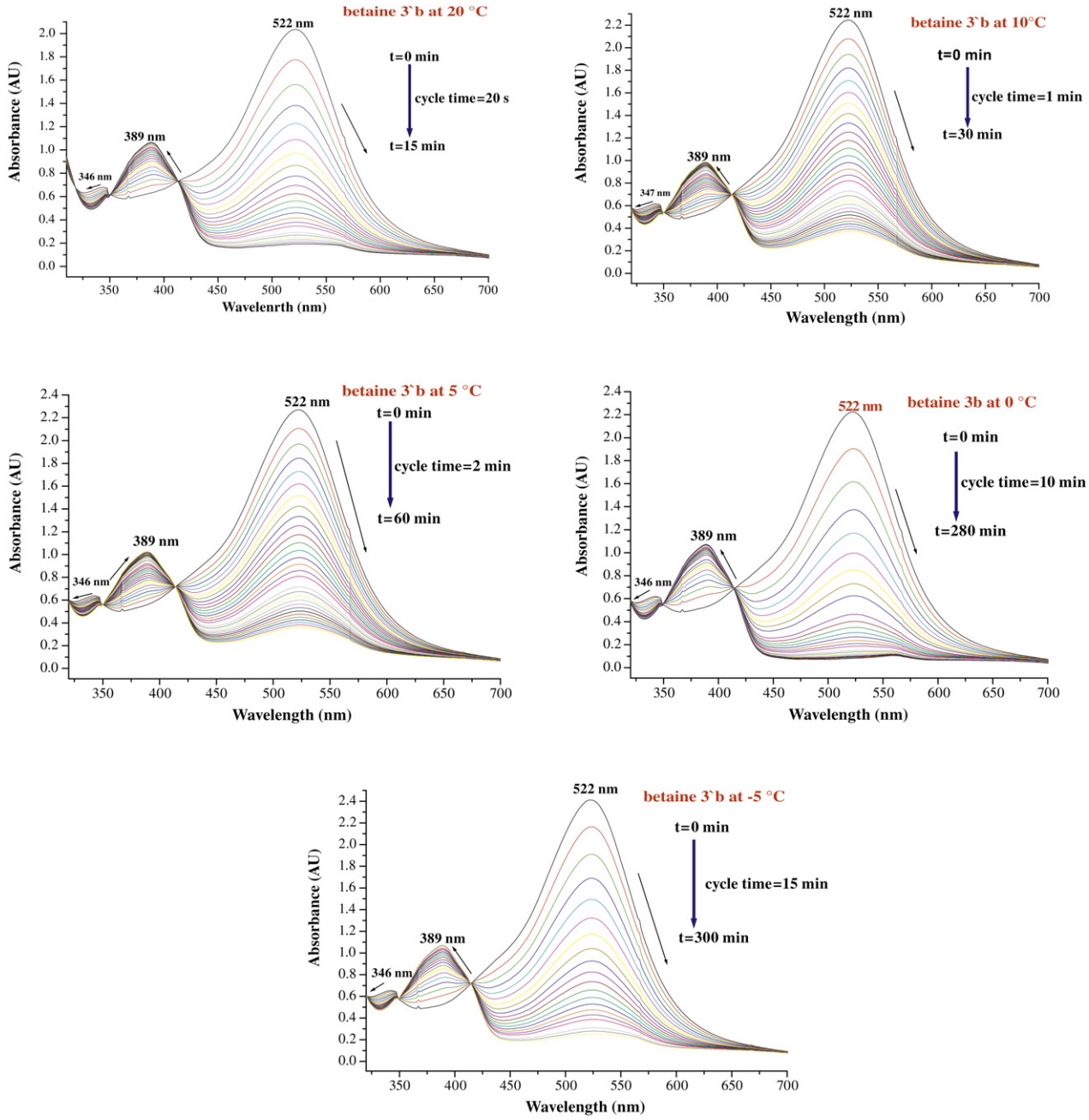

Fig. 8. Temperature-dependence effect on the half-life time of betaine **3′b** recorded from scan kinetics at different temperatures in CH_2Cl_2 solution ($c=1\times10^{-4}$ mol/L).

Irradiation of DHIs 3a-f with polychromatic light led to ring opened betaines (Figs. 6 and 7). The kinetic of the thermal 1,5-electrocyclic ring-closure reaction was studied by using a multichannel FT-UV–vis spectrophotometer (Figs. 6 and 7).

The kinetic measurements could be detected by both spectra scan (Fig. 6) and time dependent decay measurements (Fig. 7) at ambient temperature and showed that the half-lives of the colored betaines **3′a**–**f** are in second domain and range between 43 and 2700 s (Table 3, Fig. 6, 7). A highly pronounced increase in the half-lives of the betaines bearing mono and dialkyl substituted pyridazine moiety (**3′b**, **c**, **f**) by approximately a factor of 2–27 is noted compared to the non-substituted pyridazine **3′a** as well as the dihalo-substituted betaines **3′d**, **e**. This increase in the half-lives may be attributed to the stabilization of the positive charge on the betaine structures by hyperconjugation brought about by the electron donating alkyl groups. Further, it is conceivable that the proximity of the alkyl substituents to the reacting center on the pyridazine moiety hinders electrocyclization.

A noticeable decrease in the half-lives of the betaines **3′d**, **e** by approximately a factor of 1.5–2.4 was observed. The tuning of the absorption maxima and kinetic properties (Fig. 7) by manipulating substitution on the fluorene (region A) as well as on the pyridazine (region C) to find the optimal combination is fundamental and may be utilized to tailor photochromic materials to suit the requirements of specific applications.

*2.3.3. Temperature-dependence effect on the kinetics of the thermally reversible 1,5-electrocyclization of the betaines **3′a**–**f** to their corresponding DHIs **3a**–**f** in dichloromethane solution.* In order to examine the effect of temperature on the thermally reversible 1,5-electrocyclization of betaines **3′a**–**f**, FT-UV–vis spectrophotometer with temperature controller was concurrently used with sample irradiation with polychromatic light.[27–29]

Thus, irradiation of DHIs **3a**–**f** at temperatures ranging from −5 to 25 °C with simultaneous measurement of the back-reaction kinetics at the applied temperature led to different rate contacts (k)

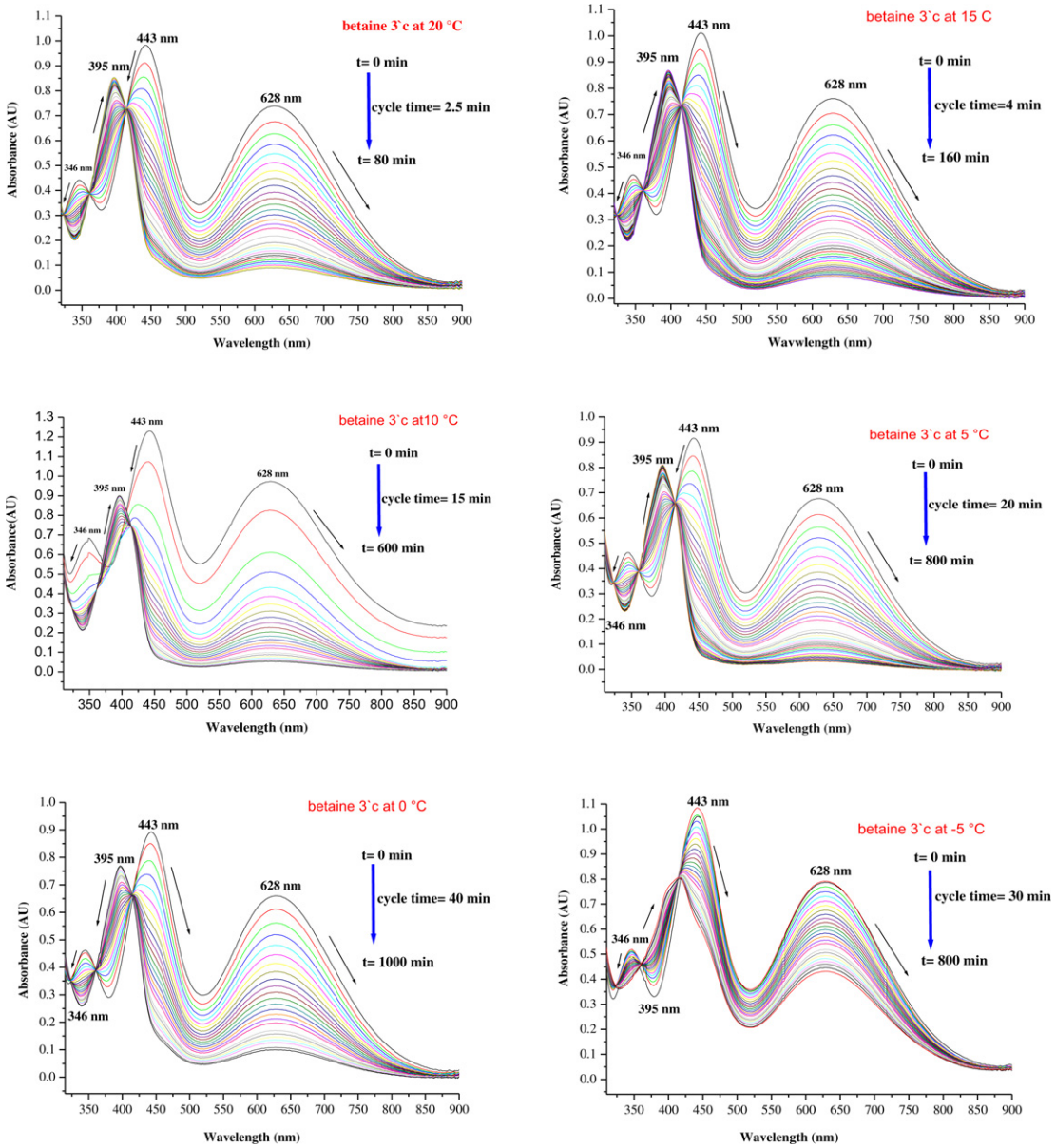

Fig. 9. Temperature-dependence effect on the half-life time of betaine **3′c** recorded from scan kinetics at different temperatures in CH_2Cl_2 solution ($c=1\times10^{-4}$ mol/L).

and half-lives. It is clear from the data summarized in Table 4 that a drastic increase in the half-lives of the betaines under investigation accompanied the corresponding decrease in the temperature (Figs. 8–10).

Table 4
Values of temperature-dependence effect on the half-life time of betaine **3′a**–**f** recorded from scan kinetics at different temperatures

Betaine	$t_{1/2}$ (25 °C)	$t_{1/2}$ (20 °C)	$t_{1/2}$ (15 °C)	$t_{1/2}$ (10 °C)	$t_{1/2}$ (5 °C)	$t_{1/2}$ (0 °C)	$t_{1/2}$ (−5 °C)
3′a	102	133	171	265	320	389	465
3′b	250	331	482	691	912	1023	1263
3′c	2700	3360	3649	3798	4036	4684	4931
3′d	67	79	93	146	176	201	257

Interestingly, the decrease in temperature has been accompanied with an increased quantum yield (generation of more betaine molecules), which resulted in significant increase in the absorbance as presented in Fig. 10.

2.3.4. Thin film measurements. It is conceivable that photochromic compounds will find wide utility in thin film application and smart windows. A required characteristic of the photochromic materials is that they should be sensitive and show ring-opening and coloration upon irradiation even with daylight. Fortunately, the present target photochromic DHIs showed these interesting photochromic properties not only in solution but also in polymer matrix. These properties were exploited to introduce such compounds as dopants to polymethyl methaacrylate (PMMA) in low concentration (2×10^{-4} mol/L) in chloroform. The evaporation method for formation of the thin film containing the photochromic DHI was used. Thus, the preparation method of the thin film on glass is summarized as follows: the slide substrates, glass standard microscope slide of thickness 1 mm, were carefully cleaned ultrasonically in acetone and then rinsed with deionized water. Dip-coated films were prepared by immersion of glass slide substrates into a chloroform solution containing the photochromic DHI **3a** doped with PMMA for approximately 1 min and then the substrate pulled up with rate of 2 mm/min using dip coating system (LayerBuilder KSV instruments LTD). The thickness was measured by Dektak150 profiler.

The transmittance, T(λ), and reflectance, R(λ), spectra of the films were measured at normal incidence and at an incident angle of 5°, respectively (Fig. 11).

The measurements were acquired in air and at room temperature in the spectral range of 190–1000 nm by using a computer aided

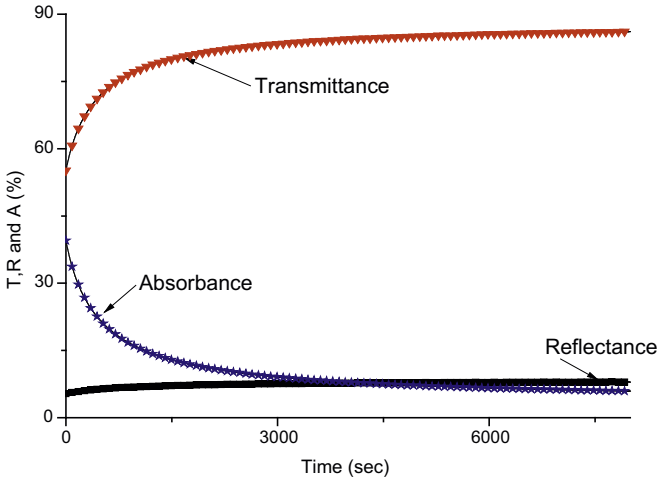

Fig. 11. Kinetic measurement of thermal fading of betaine **3′a** in PMMA thin film.

double-beam spectrophotometer (Shimadzu 3150 UV–vis–NIR) with a resolution of 0.1 nm. The condition of the surface microstructure was observed by atomic force microscopy (AFM; Veeco CP-II) in non-contact mode with Si tips at a scan rate 1 Hz. Photocolouration experiments on the photochromic films were carried out using polychromatic light with Blak-Ray lamp model UVL-56 with wavelength range of 500–1000 nm with intensity of 300 mW/cm^2 at the exposure. The photochromic samples were irradiated with a 365 nm, 100 W, B-100AP UV lamp from UVP, giving a UV-light intensity on the sample of 8.9 mW/cm^2. The film thickness was found to be 11.8 μm.

Fig. 12 shows an increase in the thermal stability for the back reaction of betaine **3′a** in the thin film by a factor of 2500 times compared with its half-life in dichloromethane solution. Eventually and as shown in Fig. 13, complete recovery of the DHI is obtained following the thermal back reaction of the betaine **3′a** in polymer doped matrix. This will help this family to find interesting applications, not only in solution, but also in solid state films and smart windows.

It is observed that by increasing the irradiation time of the photochromic thin film, the transmittance of the colored form increased and that of the closed form continued decreasing until complete conversion of the colored form was reached. This observation was detected (Fig. 12) by measuring the UV–vis spectra following various irradiation times.

In order to investigate the surface morphology of the film, AFM images in non-contact mode with a scan area of 5 μm×5 μm were recorded. The AFM micrograph (Supplementary data) revealed that

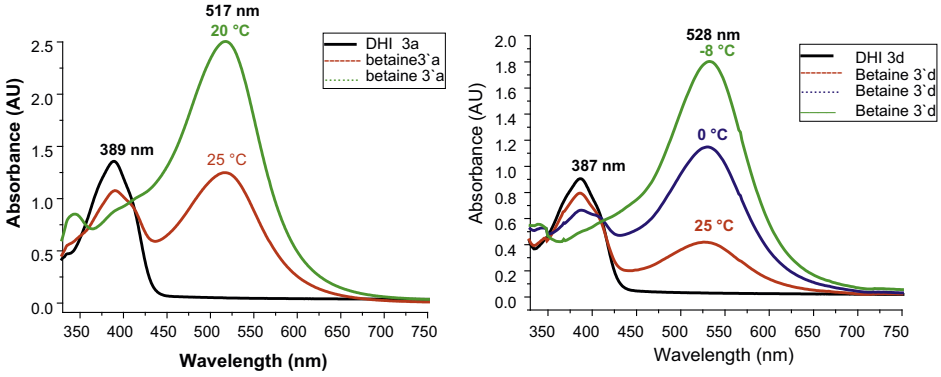

Fig. 10. Temperature-dependence effect on the thermally irreversible quantum yield and absorbance of betaine **3′a**, **d** recorded from scan kinetics at different temperatures in CH_2Cl_2 solution ($c=1\times10^{-4}$ mol/L).

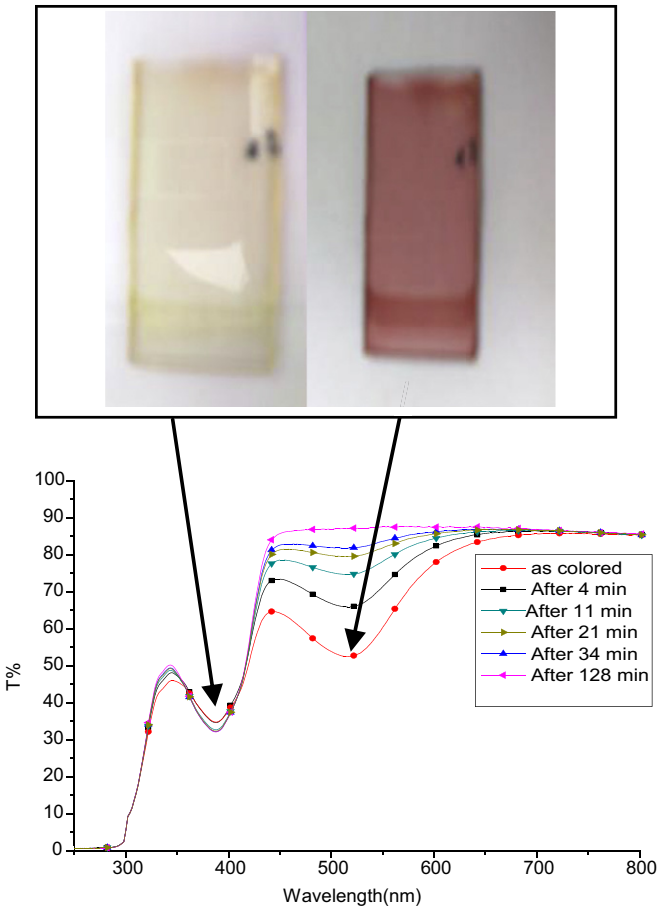

Fig. 12. The spectral transmittance for thermal fading of the colored betaine **3′a** in thin film at different time after photocoloration of DHI **3a** doped PMMA.

the film is uniform having a compact microstructure with a very smooth surface. Also, a few holes or cavities of submicron dimension are distributed over the smooth homogeneous surface. However, in spite of their presence, the film transmittance remains high. This interesting AFM image with smooth formation will help this family of compounds find industrial applications.

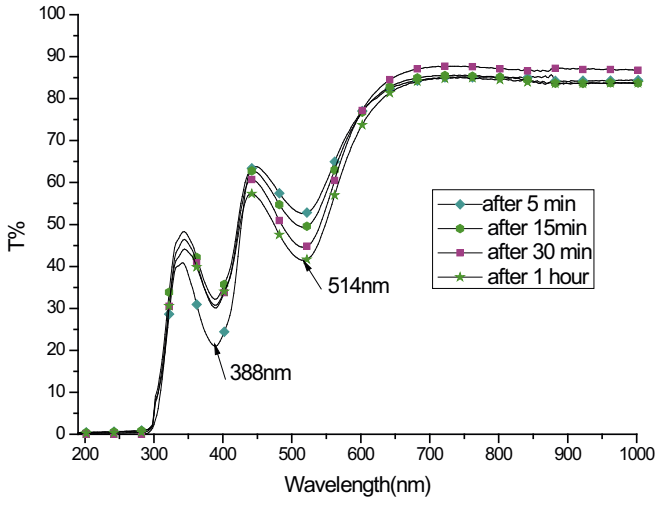

Fig. 13. The spectral transmittance for thermal fading of the colored betaine **3′a** in thin film doped PMMA at different time after photocoloration of DHI **3a**.

3. Conclusion

In summary, several novel photochromic compounds related to the interesting thermally reversible dihydroindolizines (DHIs) have been synthesized. Their chemical structures were assigned by means of spectroscopic and analytical tools. Interesting photochromic behavior in solution and in thin film was observed. One of the most pronounced properties is the structure-photochromic properties relationship, which will assist in tuning the chemical structure of the DHI skeleton toward many applications. The dependence of the thermally reversible 1,5-electrocyclization of betaines on temperature change is the most promising phenomena in this regard. Indeed, the chemical and thermal stability of the investigated betaines in polymer (PMMA) will open a new era for application of this family of compounds.

4. Experimental

4.1. General

Most of the solvents used are anhydrous and were dried according to standard procedures. Photolysis was carried out in the photochemical reactor of Schenck made from Pyrex (l>290 nm).[3,30] The source of irradiation was a high pressure mercury lamp HPK 125 W from Philips. Solutions to be photolyzed were flushed with dry nitrogen for 30 min before switching on the photolysis lamp. The heterocyclic bases used were prepared according to reported methods. The progress of the reaction and the purity of the isolated products were monitored using thin layer chromatography (TLC) and NMR. Separation and purification of all synthesized photochromic materials were carried out using column chromatography (80 cm length×2 cm diameter, silica gel) with dichloromethane as eluent. Irradiation of the cuvettes for UV–vis and Kinetic UV–vis were carried out using Ivoclar lamp (Ivoclar-ledition. 100–240 V with light intensity of 600 mW/cm^2). Melting points were measured on Büchi (Smp-20) melting point apparatus. The studied solutions for UV–vis and kinetics were prepared in concentration of 1×10^{-4} mol/L in dichloromethane solution. For thin film measurements, the slide substrates, glass standard microscope slide of thickness 1 mm, were carefully cleaned ultrasonically in acetone and then rinsed with deionized water. Dip-coated films were prepared by immersion of glass slide substrates into the polymer doped photochromic material for approximately 1 min and then the substrate pulled up with rate of 2 mm/min using dip coating system (Layer Builder KSV instruments LTD). The thickness was measured by Dektak150 profiler.

The transmittance T(λ), and reflectance R(λ) spectra of the films were measured at normal incidence and at an incident angle of 5°, respectively. The measurements were acquired in air and at room temperature in the spectral range of 190–1000 nm by using a computer aided double-beam spectrophotometer (Shimadzu 3150 UV–VIS–NIR) with a resolution of 0.1 nm. The condition of the surface microstructure was observed by atomic force microscopy (AFM; Veeco CP-II) in non-contact mode with Si tips at a scan rate 1 Hz. Photocoloration experiments on the photochromic films were carried out using A UV lamp. Photochromic samples doped with polymer were irradiated with a 365 nm, 100 W, B-100AP UV lamp from UVP, giving an UV-light intensity on the sample of 8.9 mW/cm^2. Photocoloration was carried out using Blak-Ray lamp model UVL-56 with a wavelength range of 500–1000 nm with an intensity of 300 mW/cm^2 at the exposure. Thickness was found to be 11.8 μm. The fluorene spirocyclopropene precursors **1a**–**c** were synthesized with some modifications to the published patented methods.[13,14,23,28,29]

4.2. Synthesis of substituted dimethyl 4a′*H*-spiro[fluorene-9,5′-pyrrolo[1,2-*b*]pyridazine]-6′,7′-dicarboxylate dihydroindolizines 3a–f (General procedure)

To a mixture of spirocyclopropenes **1a**–**c** (25 mmol) in 100 mL freshly dried ether at room temperature was added under dry N_2 and in absence of light, substituted pyridazines **2a**–**d** (26 mmol). The mixture was stirred at room temperature for 24 h (TLC-monitored). The ether was removed under reduced pressure and the pure products were obtained after being subjected at least twice to column chromatography on silica gel using dichloromethane as eluent to afford the photochromic products **3a**–**f** in low to moderate yields. Experimental details and full characterizations of the new synthesized DHIs **3a**–**f** are described below:

4.2.1. Dimethyl 4a′H-spiro[fluorene-9,5′-pyrrolo[1,2-b]pyridazine]-6′,7′ dicarboxylate ***3a***. Yield (386 mg, 40%) as pale yellow solid, mp=124–126 °C; [Found: C, 71.6; H, 4.5; N, 7.5. $C_{23}H_{18}N_2O_4$ requires 71.5; H, 4.7; N, 7.3]; R_f (CH_2Cl_2) 0.51; ν_{max} (KBr) 3014, 2951, 1750, 1727, 1597, 1519 cm^{-1}; δ_H (400 MHz, $CDCl_3$) 7.75–7.73 (2H, d, *J*=7.6 Hz, Ph), 7.59–7.57 (1H, d, *J*=7.6 Hz, Ph), 7.51–7.49 (1H, d, *J*=7.6 Hz, Ph), 7.32–7.43 (3H, m, Ph), 7.26–7.24 (1H, dd, *J*=7.5, 1.2 Hz, Ph), 6.95–6.94 (1H, dd, *J*=3.5, 1.6 Hz, 6′H), 5.67–5.69 (1H, ddd, *J*=9.8, 3.3, 2.7 Hz, 7′H), 5.30–5.29 (1H, d, *J*=2.4 Hz, 8′aH), 5.00 (1H, dt, *J*=10.1, 1.8 Hz, 8′H), 4.03 (s, 3H, 2′-CH_3), 3.32 (s, 3H, 2′-CH_3); δ_C (100.6 MHz, $CDCl_3$) 163.4, 161.8, 149.4, 146.5, 141.6, 140.9, 140.5, 138.5, 128.6, 128.3, 127.8, 127.2, 126.0, 124.7, 123.5, 120.2, 119.9, 118.4, 106.1, 65.5, 63.4, 53.3, 51.1; *m*/*z* (EI) 286.16 [M^+], 327.1 (4), 279.1 (10), 167 (34), 149.3 (100), 83.6 (43), 57.0 (76%).

4.2.2. Dimethyl 2′-methyl-4a′H-spiro[fluorene-9,5′-pyrrolo[1,2-b]pyridazine]-6′,7′-dicarboxylate ***3b***. Yield (429 mg, 43%) as pale yellow solid, mp=189–191 °C; [Found: C, 72.2; H, 4.9; N, 7.3. $C_{24}H_{20}N_2O_4$ requires C, 72.1; H, 5.0; N, 7.1%]; R_f (CH_2Cl_2) 0.52; ν_{max} (KBr) 3106, 2991, 1720, 1760, 1600, 1448 cm^{-1}; δ_H (400 MHz, $CDCl_3$) 7.73–7.71 (2H, d, *J*=7.6 Hz, Ph), 7.59–7.57 (1H, d, *J*=7.2 Hz, Ph), 7.50–7.49 (1H, d, *J*=7.6 Hz, Ph), 7.42–7.34 (3H, m, Ph), 7.24–7.21 (1H, td, *J*=7.5, 1.1 Hz, CH-arom.), 5.64–5.62 (1H, dd, *J*=9.9, 2.6 Hz, 7′H), 5.16–5.15 (1H, t, *J*=2.4 Hz, 8′aH.), 5.09–5.07 (1H, dd, *J*=9.8, 2.1 Hz, 8′H), 4.03 (3H, s, 3′-CH_3), 3.30 (3H, s, 2′-CH_3), 2.01 (3H, s, 6′-CH_3); δ_C (100.6 MHz, $CDCl_3$) 163.6, 162.1, 149.8, 147.4, 147.0, 141.6, 141.5, 140.4, 128.5, 128.2, 127.8, 127.2, 127.1, 124.8, 123.6, 121.1, 120.1, 119.8, 104.1, 64.9, 62.9, 53.2, 51.0, 21.1; *m*/*z* (EI) 400.13 [M^+, 100], 247.0 (39), 189.0 (64), 176.0 (24), 94.0 (14%).

4.2.3. Dimethyl 2′-heptyl-4a′-methyl-4a′H-spiro[fluorene-9,5′-pyrrolo[1,2-b]pyridazine]-6′,7′-dicarboxylate ***3c***. Yield (337 mg, 27%), as yellow solid, mp=122–120 °C; [Found: C, 74.5; H, 5.7; N, 5.50. $C_{24}H_{20}N_2O_4$ requires C, 74.7; H, 6.9; N, 5.6%]; R_f (CH_2Cl_2) 0.55; ν_{max} (KBr) 3051, 29,501,749, 1697, 1591, 1519 cm^{-1}; δ_H (400 MHz, $CDCl_3$) 7.72–7.70 (1H, d, *J*=7.5 Hz, Ph), 7.67–7.65 (1H, d, *J*=7.6 Hz, Ph), 7.59–7.58 (1H, d, *J*=7.6 Hz, 1H, Ph), 7.46–7.47 (1H, d, *J*=7.6 Hz, CH-arom.), 7.40–7.37 (1H, td, *J*=7.5, 1.0 Hz, Ph), 7.34–7.31 (1H, td, *J*=7.5, 1.0 Hz, Ph), 7.29–7.26 (1H, td, *J*=7.5, 1.1 Hz, Ph), 7.20–7.17 (1H, td, *J*=7.5, 1.1 Hz, Ph), 5.49–5.47 (1H, d, *J*=9.8 Hz, 7′H), 5.04–5.01 (1H, d, *J*=9.8 Hz, 8′H), 4.02 (3H, s, 3′-CH_3), 3.32 (3H, s, 2′-CH_3), 2.28–2.28 (2H, t, *J*=7.7 Hz, 6′a-CH_2), 1.47 (3H, s, 8′a-CH_3), 1.53–1.48 (2H, m, 6′b-CH_2), 1.34–1.19 (8H, m, 6′-c, d, e, f (CH_2)$_4$), 0.91–0.89 (3H, t, *J*=6.9 Hz, 6′-g-CH_3); δ_C (100.6 MHz, $CDCl_3$) 164.1, 162.2, 150.5, 149.3, 143.2, 142.8, 142.0, 140.1, 133.4, 128.2, 128.1, 127.0, 126.9, 126.6, 124.8, 120.0, 119.7, 117.6, 102.0, 66.9, 66.6, 53.1, 50.9, 34.9, 31.7, 29.1, 29.0, 27.1, 22.6, 22.5, 14.1 ppm; *m*/*z* (EI) 498.61 [M^+, 100], 439.2 (18), 247.0 (34), 189.0 (34), 94.1 (12%).

4.2.4. Dimethyl 2,7-dichloro-4a′H-spiro[fluorene-9,5′-pyrrolo[1,2-b]pyridazine]-6′,7′-dicarboxylate ***3d***. Yield (431 mg, 38%) as pale yellow solid, mp=130–128 °C; [Found: C, 60.7; H, 3.5; Cl, 15.6; N, 6.2. $C_{23}H_{16}Cl_2N_2O_4$ requires C, 60.7; H, 3.5; Cl, 15.6; N, 6.2%]; R_f (CH_2Cl_2) 0.50; ν_{max} (KBr) 3180, 2951, 1751, 1701, 1599, 1519, 1193 cm^{-1}; δ_H (400 MHz, $CDCl_3$) 7.63–7.60 (1H, d, *J*=8.1 Hz, Ph), 7.62–7.59 (1H, d, *J*=8.1 Hz, Ph), 7.57–7.58 (1H, d, *J*=1.9 Hz, Ph), 7.43–7.42 (1H, d, *J*=1.9 Hz, Ph), 7.39–7.36 (1H, dd, *J*=8.1, 1.9 Hz, Ph), 7.38–7.36 (1H, dd, *J*=8.1, 1.9 Hz, Ph), 7.01–6.98 (1H, dd, *J*=3.4, 1.6 Hz, 6′H), 5.77–5.79 (1H, ddd, *J*=9.8, 3.3, 2.8 Hz, 7′H), 5.25–5.22 (1H, t, *J*=2.4 Hz, 8′aH), 5.07–5.02 (1H, dt, *J*=9.8, 1.8 Hz, 8′H), 4.03 (3H, s, 3′-CH_3), 3.38 (3H, s, 2′-CH_3); δ_C (100.6 MHz, $CDCl_3$) 163.0, 161.3, 149.8, 148.5, 142.7, 139.0, 138.9, 138.0, 133.9, 133.2, 129.2, 128.8, 125.3, 125.0, 124.1, 121.2, 120.8, 119.0, 104.8, 65.2, 63.2, 53.4, 51.3 ppm; *m*/*z* (%) 454.05 [M^{-1}, 88], 420.1 (78), 315.1 (28), 257.0 (46), 81.1 (100%).

4.2.5. Dimethyl 2,7-dibromo-4a′H-spiro[fluorene-9,5′-pyrrolo[1,2-b]pyridazine]-6′,7′-dicarboxylate ***3e***. Yield (474 mg, 35%) as pale yellow solid, mp=136–134 °C; [Found: C, 50.5; H, 3.0; N, 5.0. $C_{23}H_{16}Br_2N_2O_4$ requires C, 50.7; H, 3.00; N, 5.2%]; R_f (CH_2Cl_2) 0.51; ν_{max} (KBr) 3170, 2951, 1751, 1701, 1599, 1519, 1195 cm^{-1}; δ_H (400 MHz, $CDCl_3$) 7.73–7.70 (1H, d, *J*=1.5 Hz, Ph), 7.59–7.48 (5H, m, Ph), 7.00–6.98 (1H, dd, *J*=3.4, 1.5 Hz, 6′H), 5.76–5.74 (1H, ddd, *J*=9.8, 3.4, 2.8 Hz, 7′H), 5.25–5.21 (1H, t, *J*=2.3 Hz, 8′H), 5.05–5.02 (1H, dt, *J*=9.8, 1.9 Hz, 8′aH), 4.03 (3H, s, 3′-CH_3), 3.38 (3H, s, 2′-CH_3); δ_C (100.6 MHz, $CDCl_3$) 162.9, 161.2, 149.7, 148.6, 142.7, 139.4, 138.9, 138.4, 132.1, 131.6, 127.7, 126.9, 125.2, 122.0, 121.6, 121.3, 121.2, 119.0, 104.6, 65.2, 63.1, 53.4, 51.3 ppm; *m*/*z* (%) 541.21[M^{-2}, 100], 525.8 (24), 481.8 (14), 388.1 (8), 279.5 (13), 163.0 (20%).

4.2.6. Dimethyl 2,7-dibromo-2′,3′,4′,4a′-tetramethyl-4a′H-spiro[fluorene-9,5′-pyrrolo[1,2-b]pyridazine]-6′,7′-dicarboxylate ***3f***. Yield (392 mg, 29%) as yellow solid; mp=167–165 °C; [Found: 53.8; H, 4.1; N, 4.5. $C_{27}H_{24}Br_2N_2O_4$ requires C, 54.00; H, 4.00; N, 4.7%]; R_f (CH_2Cl_2) 0.56; ν_{max} (KBr) 3175, 2949, 1735, 1681, 1591, 1546, 1178 cm^{-1}; δ_H (400 MHz, $CDCl_3$) 7.76–7.73 (1H, d, *J*=1.6 Hz, Ph), 7.62–7.60 (1H, d, *J*=1.6 Hz, Ph), 7.60–7.56 (1H, d, *J*=8.1 Hz, Ph), 7.54–7.52 (1H, dd, *J*=8.1, 1.6 Hz, Ph), 7.51–7.48 (1H, d, *J*=8.1 Hz, Ph), 7.48–7.45 (1H, dd, *J*=8.1, 1.6 Hz, Ph), 4.01 (3H, s, 3′-CH_3), 3.34 (3H, s, 3H, 2′-CH_3), 2.07 (3H, s, 6′-CH_3), 1.57 (3H, s, 7′-CH_3), 1.56 (3H, s, 8′a-CH_3), 0.73 (3H, s, 8′-CH_3); δ_C (100.6 MHz, $CDCl_3$) 163.6, 162.0, 150.8, 149.0, 147.0, 146.3, 140.3, 138.5, 138.2, 131.6, 131.4, 129.9, 127.4, 122.7, 121.4, 121.2, 121.1, 121.0, 101.6, 71.0, 66.2, 53.2, 51.0, 20.3, 19.5, 13.4, 12.6 ppm; *m*/*z* (%) 602.01 [M^{+2}, 100], 543.9 (80), 404.9 (22), 346.9 (34), 187 (36%).

Acknowledgements

S.A.A. is highly indebted to the University of Saarland and Alexander von Humboldt foundation (AvH), Germany for their financial support of this work and their chemicals and instrumentation donations. Also, the authors are highly indebted to Taibah University and the deanship of scientific research for the partially support of this work through the funded project no. 479/430.

Supplementary data

Supplementary data associated with this article can be found, in the online version, at doi:10.1016/j.tet.2011.06.092.

References and notes

1. (a) Bouas-Laurent, H.; Dürr, H. *Pure Appl. Chem.* **2001**, *73*, 639–665; (b) Dorion, G. H.; Wiebe, A. F. *Photochromism*; Focal: New York, NY, 1970; (c) *Photochromism*; Brown, G. H., Ed.; Wiley: New York, NY, 1971; (d) *Photochromism: Molecules and Systems*; Dürr, H., Bouas-Laurent, H., Eds.; Elsevier: Amsterdam, 1990; (e) *Organic Photochromic and Thermochromic Compounds*; Crano, G. C., Guglielmetti, R., Eds.; Plenum: New York, NY, 1999; (f) *Applied Photochromic*

Polymer Systems; McArdle, C. B., Ed.; Blackie: Glasgow, 1992; (g) *Photo-Reactive Materials for Ultrahigh Density Optical Memory*; Irie, M., Ed.; Elsevier: Amsterdam, 1994.
2. (a) Guglielmeti, R.; Samat, A. Proceedings of the First International Symposium on Organic Photochromism *Mol. Cryst. Liq. Cryst.* **1994**, 3–220; (b) Irie, M. In *Molecular Switches*; Feringa, B. L., Ed.; Wiley-VCH: Weinheim, 2001; pp 37–60; (c) Irie, M. In *Organic Photochromic and Thermochromic Compounds*; Crano, J. C., Gugielmetti, R. J., Eds.; Plenum: New York, NY, 1999; Vol. 1, pp 207–221.
3. (a) Mizokuro, T.; Mochizuki, H.; Kobayashi, A.; Horiuchi, S.; Yamamoto, T. *Chem. Mater.* **2004**, *16*, 3469–3475; (b) Mizokuro, T.; Mochizuki, H.; Xiaoliang, M.; Horiuchi, S.; Tanaka, T. *Jpn. J. Appl. Phys.* **2003**, *42*, 983–985; (c) Tian, H.; Chen, B.; Tu, H.; Müllen, K. *Adv. Mater.* **2002**, *14*, 918–923; (d) Irie, M.; Fukaminato, T.; Sasaki, T.; Tamai, N.; Kawai, T. *Nature* **2002**, *420*, 759–760; (e) Norsten, T. B.; Branda, N. R. *J. Am. Chem. Soc.* **2001**, *123*, 1784–1785.
4. (a) Hirshberg, Y.; Fischer, E. *J. Chem. Soc.* **1953**, 629–636; (b) Persano, L.; Mele, E.; Athanassiou, A.; Cingolani, R.; Psignano, D. *Chem. Mater.* **2006**, *18*, 4171–4175; (c) Tanaka, M.; Kamada, K.; Ando, H.; Kitagaki, T.; Shibutani, Y.; Yajima, K. *Chem. Commun.* **1999**, 1453–1454; (d) Norsten, T. B.; Branda, N. R. *Adv. Mater.* **2001**, *13*, 347–349.
5. (a) Tsivgoulis, G.; Lehn, J.-M. *Angew. Chem., Int. Ed. Engl.* **1995**, *34*, 1119–1122; (b) Tsujioka, T.; Hamada, Y.; Shibata, K. *Appl. Phys. Lett.* **2001**, *78*, 2282–2284; (c) Wojtyk, J. T.; Buncel, E.; Kazmaier, P. M. *Chem. Commun.* **1998**, 1703–1704; (d) Tanaka, M.; Nakamura, M.; Salhin, M. A. A.; Ikeda, T.; Kamada, K.; Ando, H. *J. Org. Chem.* **2001**, *66*, 1533–1537.
6. (a) Kawai, T.; Kunitake, T.; Irie, M. *Chem. Lett.* **1999**, 905–906; (b) Bertarelli, C.; Bianco, A.; D'Amore, F.; Gallazzi, M. C.; Zerbi, G. *Adv. Funct. Mater.* **2004**, *14*, 357–363; (c) Kim, M. S.; Maruyama, H.; Kawat, T.; Irie, M. *Chem. Mater.* **2003**, *15*, 4539–4543.
7. (a) Biteau, J.; Chaput, F.; Lahlil, K.; Boilot, J.-P.; Tsivgoulis, G. M.; Lehn, J.-M.; Darracq, B.; Marois, C.; Lévy, Y. *Chem. Mater.* **1998**, *10*, 1945–1950; (b) van Delden, R. A.; ter Wiel, K. K. J.; Feringa, B.-L. *Chem. Commun.* **2004**, 200–201; (c) Feringa, B.-L.; van Delden, R. A.; ter Wiel, M. K. J. In *Molecular Switches*; Feringa, B.-L., Ed.; Wiley-VCH: Weinheim, 2001; pp 123–164; (d) Murguly, E.; Norsten, T. B.; Branda, N. R. *Angew. Chem., Int. Ed.* **2001**, *40*, 1752–1755.
8. (a) Kim, E.; Choi, Y.-K.; Lee, M.-H. *Macromolecules* **1999**, *32*, 4855–4860; (b) Moniruzzaman, M.; Sabey, C. J.; Fernando, G. F. *Macromolecules* **2004**, *37*, 2572–2577; (c) Lucas, L. N.; van Esch, J.; Kellogg, R. M.; Feringa, B.-L. *Chem. Commun.* **2001**, 759–760; (d) Kang, J. W.; Kim, J.-J.; Kim, E. *Appl. Phys. Lett.* **2002**, *80*, 1710–1713; (e) Wang, C.; Batsanov, A. S.; Bryce, M. R.; Sage, I. *Synthesis* **2003**, *13*, 2089–2095; (f) Wang, C.; Pålsson, L.-O.; Batsanov, A. S.; Bryce, M. R. *J. Am. Chem. Soc.* **2006**, *128*, 3789–3799.
9. (a) Kang, J. W.; Kim, J.-J.; Kim, E. *Opt. Mater.* **2002**, *21*, 543–548; (b) Myles, A. J.; Branda, N. R. *Adv. Funct. Mater.* **2002**, *12*, 167–173; (c) Hugel, T.; Holland, N. B.; Cattani, A.; Moroder, L.; Seitz, M.; Gaub, H. E. *Science* **2002**, *296*, 1103–1106.
10. (a) Alonso, M.; Reboto, V.; Guiscardo, L.; San Martin, A.; Rodriguez-Cabello, J. C. *Macromolecules* **2000**, *33*, 9480–9482; (b) Wigglesworth, T. G.; Myles, A. J.; Branda, N. R. *Eur. J. Org. Chem.* **2005**, 1233–1238.
11. Peters, A.; Vitols, C.; McDonald, R.; Branda, N. R. *Org. Lett.* **2002**, *5*, 1183–1186.
12. (a) Kalyanasundaram, K.; Grätzel, M. *Coord. Chem. Rev.* **1998**, 347–414; (b) Argazzi, R.; Bignozzi, C. A.; Heimer, T. A.; Castellano, F. N.; Meyer, G. J. *Inorg. Chem.* **1994**, *33*, 5741–5749.
13. (a) Dürr, H. *Angew. Chem.* **1989**, *101*, 427–445; *Int. Ed. Engl.* **1989**, *28*, 413–438; (b) Dürr, H. *Wiss. Zeitschr. TH Leuna-Merseburg* **1984**, *26*, 664–671; (c) Dürr, H.; Gross, H.; Zils, K. D. Deutsche Offenlegungs Schrift Pat. 1983, 32 20 275 A1. (d) Dürr, H.; Jönsson, H. P.; Scheidhauer, P.; Münzmay, T.; Spang, P. Deutsche Offenlegungs Schrift Pat. 1985, 3521432 5.
14. (a) Dürr, H.; Janzen, K. P.; Thome, A.; Braun, B.; Deutsche Offenlegungs Schrift Pat. 1988, 3521432 5. (b) Dürr, H.; Gross, H.; Zils, K. D.; Hauck, G.; Hermann, H. *Chem. Ber.* **1983**, *116*, 3915–3925; (c) Dürr, H.; Spang. P. Deutsche Offenlegungs Schrift Pat. 1984, 32 20 2571.
15. (a) Fromm, R.; Ahmed, S. A.; Hartmann, T.; Huch, V.; Abdel-Wahab, A. A.; Dürr, H. *Eur. J. Org. Chem.* **2001**, *21*, 4077–4080; (b) Weber, C.; Rustemeyer, F.; Dürr, H. *Adv. Mater.* **1998**, *10*, 1348–1351.
16. (a) Andreis, C.; Dürr, H.; Wintgens, V.; Valat, P.; Kossanyi, J. *Chem.—Eur. J.* **1997**, *3*, 509–516; (b) Ahmed, S. A.; Abdel-Wahab, A. A.; Dürr, H. In *CRC Handbook of Organic Photochemistry and Photobiology*, 2nd ed.; Horspool, W. M., Lenci, F., Eds.; CRC: New York, NY, 2003; Chapter 96, pp 1–25.
17. (a) Ahmed, S. A.; Hartmann, T.; Huch, V.; Dürr, H.; Abdel-Wahab, A. A. *J. Phys. Org. Chem.* **2000**, *13*, 539–548.
18. (a) Tan, Y. S.; Ahmed, S. A.; Dürr, H.; Huch, V.; Abdel-Wahab, A. A. *Chem. Commun.* **2001**, 1246–1247.
19. (a) Ahmed, S. A. *Mol. Cryst. Liq. Cryst.* **2005**, *430*, 295–300; (b) Ahmed, S. A.; Dürr, H. *Mol. Cryst. Liq. Cryst.* **2005**, *431*, 275–280.
20. (a) Ahmed, S. A. *Monatshefte für Chemie* **2004**, *135*, 1173–1188; (b) Ahmed, S. A.; Abdel-Wahab, A. A.; Dürr, H. *J. Photochem. Photobiol.* **2003**, *154*, 131–144; (c) Ahmed, S. A. *J. Phys. Org. Chem.* **2002**, *15*, 392–402.
21. (a) Ahmed, S. A. *J. Phys. Org. Chem.* **2006**, *19*, 402–414; (b) Ahmed, S. A. *J. Phys. Org. Chem.* **2007**, *20*, 564–588.
22. (a) Ahmed, S. A.; Hartmann, T.; Dürr, H. *J. Photochem. Photobiol.* **2008**, *200*, 50–56; (b) Ahmed, S. A.; Pozzo, J.-L. *J. Photochem. Photobiol.* **2008**, *200*, 57–67.
23. (a) Dürr, H. *Chimica* **1994**, 514–515; (b) Dürr, H.; Amlung, M.; Rustemeyer, F.; Tan. Y. S.; Deutsche Offenlegungs-Schrift Pat. 1998, 198, 349–408.
24. (a) Masson, J.-F.; Hartmann, T.; Dürr, H.; Booksh, K. S. *Opt. Mater.* **2004**, *27*, 435–439; (b) Terazono, Y.; Kodis, J.; Andreasson, J.; Jeong, G.; Brune, A.; Hartmann, T.; Dürr, H.; Moore, A.-L.; Moore, T. A.; Gust, D. *J. Phys. Chem.* **2004**, *108*, 1812–1814.
25. Gogritchiani, E.; Hartmann, T.; Palm, B.; Samsoniya, S.; Dürr, H. *J. Photochem. Photobiol., B* **2002**, *67*, 18–22.
26. (a) Ahmed, S. A. *Tetrahedron* **2009**, *65*, 1373–1388; (b) Ahmed, S. A. *Res. Lett. Org. Chem.* **2008**, Article ID 959372, 5 pages.
27. Kamtekar, K. T.; Wang, C.; Bettington, S.; Batsanov, A. S.; Perepichka, I. F.; Bryce, M. R.; Ahn, J. H.; Rabinal, M.; Petty, M. C. *J. Mater. Chem.* **2006**, *16*, 3823–3835.
28. Gautron, R. *Bull. Soc. Chim. Fr.* **1968**, 3200–3204.
29. (a) Hesse, M.; Meier, H.; Zeeh, B. *Spektroskopische Methoden in der Organischen Chemie*; Georg Thieme: Stuttgart, 1995; New York 185–186.
30. Schönberg, A. *Präparative Organische Photochemie*; Springer: Berlin, 1958, Chapter1.